Characterization of In Vitro Glucuronidation Clearance of a Range of Drugs in Human Kidney Microsomes: Comparison with Liver and Intestinal Glucuronidation and Impact of Albumin[S]

Katherine L. Gill, J. Brian Houston, and Aleksandra Galetin

Centre for Applied Pharmacokinetic Research, School of Pharmacy and Pharmaceutical Sciences, University of Manchester, Manchester, United Kingdom

ABSTRACT:

Previous studies have shown the importance of the addition of albumin for characterization of hepatic glucuronidation in vitro; however, no reports exist on the effects of albumin on renal or intestinal microsomal glucuronidation assays. This study characterized glucuronidation clearance ($CL_{int, UGT}$) in human kidney, liver, and intestinal microsomes in the presence and absence of bovine serum albumin (BSA) for seven drugs with differential UDP-glucuronosyltransferase (UGT) 1A9 and UGT2B7 specificity, namely, diclofenac, ezetimibe, gemfibrozil, mycophenolic acid, naloxone, propofol, and telmisartan. The impact of renal $CL_{int, UGT}$ on accuracy of in vitro-in vivo extrapolation (IVIVE) of glucuronidation clearance was investigated. Inclusion of 1% BSA for acidic drugs and 2% for bases/neutral drugs in incubations was found to be suitable for characterization of $CL_{int, UGT}$ in different tissues. Although BSA increased $CL_{int, UGT}$ in all tissues, the extent was tissue- and drug-dependent. Scaled $CL_{int, UGT}$ in the presence of BSA ranged from 2.22 to 207, 0.439 to 24.4, and 0.292 to 23.8 ml · min^{-1} · g tissue^{-1} in liver, kidney, and intestinal microsomes. Renal $CL_{int, UGT}$ (per gram of tissue) was up to 2-fold higher in comparison with that for liver for UGT1A9 substrates; in contrast, $CL_{int, UGT}$ for UGT2B7 substrates represented approximately one-third of hepatic estimates. Scaled renal $CL_{int, UGT}$ (in the presence of BSA) was up to 30-fold higher than intestinal glucuronidation for the drugs investigated. Use of in vitro data obtained in the presence of BSA and inclusion of renal clearance improved the IVIVE of glucuronidation clearance, with 50% of drugs predicted within 2-fold of observed values. Characterization and consideration of kidney $CL_{int, UGT}$ is particularly important for UGT1A9 substrates.

Introduction

Glucuronidation, via the UDP-glucuronosyltransferases (UGTs), is an important clearance mechanism for many xenobiotics and endogenous compounds (Tukey and Strassburg, 2000; Kiang et al., 2005). In vivo data indicate that the kidneys play an important role in the glucuronidation of certain drugs (Mazoit et al., 1990; Takizawa et al., 2005) and in the case of nonsteroidal anti-inflammatory drugs glucuronidation has also been linked to renal toxicity (Knights et al., 2009). Expression of certain UGT enzymes, e.g., 1A9 and 2B7, has been reported along the convoluted tubules, the loop of Henle, and collecting ducts and in the macula densa of the kidney (Gaganis et al., 2007; Lash et al., 2008); mRNA data suggest that expression of other UGTs is lower (Nishimura and Naito, 2006; Ohno and Nakajin, 2009).

Considering the importance of UGT1A9 and UGT2B7 for drug clearance, renal glucuronidation may make a substantial contribution to systemic clearance, as illustrated in the case of propofol for which the kidney contributes up to one-third of total glucuronidation (Takizawa et al., 2005). In vitro characterization of renal glucuronidation and its importance relative to liver and intestinal glucuronidation has been relatively limited (Raoof et al., 1996; Bowalgaha and Miners, 2001; Soars et al., 2001).

Previous studies have shown that UGT1A9 and UGT2B7 are competitively inhibited by free fatty acids (FFAs) released during microsomal incubation; this effect is particularly evident for linoleic and arachidonic acids (Tsoutsikos et al., 2004). In contrast, FFAs were reported to have no effect on glucuronidation via UGT1A1 or UGT1A6 (Rowland et al., 2008). Bovine serum albumin (BSA) has been used to sequester FFAs in microsomal assays and prevent inhibition of glucuronidation (Rowland et al., 2007, 2008). Addition of BSA has resulted in up to 16-fold increases in glucuronidation intrinsic clearance ($CL_{int, UGT}$) obtained either by depletion or metabolite formation in human liver microsomes (HLM), resulting in improved prediction accuracy when in vitro-in vivo extrapolation (IVIVE) of such data was performed (Rowland et al., 2008, 2009; Kilford et al., 2009; Manevski et al., 2011). Analogous to liver,

---

ABBREVIATIONS: UGT, UDP-glucuronosyltransferase; FFA, free fatty acid; BSA, bovine serum albumin; HLM, human liver microsomes; IVIVE, in vitro-in vivo extrapolation; HKM, human kidney microsomes; HIM, human intestinal microsomes; MPA, mycophenolic acid; LC, liquid chromatography; MS/MS, tandem mass spectrometry.

arachidonic and linoleic acids represent two of the most abundant FFAs in renal and intestinal tissue (Soydan et al., 1996; Hoffmann et al., 2005; Rowland et al., 2007). However, to date there have been no studies assessing the effects of BSA on glucuronidation in human kidney (HKM) or intestinal (HIM) microsomes.

In vitro glucuronidation is influenced by assay conditions, and high intersubject variability has been observed for many UGTs, including UGT1A9 and UGT2B7 (Fisher et al., 2000; Soars et al., 2003; Court, 2010). UGT expression is not consistent throughout the kidney or intestine, and the region used for microsomal preparation will affect glucuronidation capacity (Gaganis et al., 2007; Lash et al., 2008; Bellemare et al., 2011). At present, absolute abundance data are available for only a few UGTs, primarily quantified in liver tissue and from a limited number of donors (Harbourt et al., 2012; Ohtsuki et al., 2012; Schaefer et al., 2012). In addition, UGT mRNA/protein expression data are often inconsistent among studies and are associated with high variability (Izukawa et al., 2009; Milne et al., 2011). IVIVE studies have concentrated on hepatic glucuronidation and have consistently underpredicted in vivo clearance (Boase and Miners, 2002; Miners et al., 2006; Cubitt et al., 2009; Kilford et al., 2009) but arguably no more than predictions of cytochrome P450 clearance (Hallifax et al., 2010). There have been few attempts to include extrahepatic glucuronidation in IVIVE (Soars et al., 2002; Al-Jahdari et al., 2006); lack of consideration of extrahepatic glucuronidation, differences in scaling factors, and in vitro assay conditions may contribute to the underprediction trend observed.

The aim of this study was to characterize and compare glucuronidation clearance in the kidney, liver, and intestine for seven selected drugs, namely diclofenac, ezetimibe, gemfibrozil, mycophenolic acid (MPA), naloxone, propofol, and telmisartan. The drugs selected covered a range of physicochemical properties, differing specificity for UGT1A9 and/or UGT2B7 and formed both acyl and phenolic glucuronides. Unbound intrinsic glucuronidation clearance ($CL_{int, u, UGT}$) was characterized in alamethicin-activated HLM, HKM, and HIM under standardized in vitro conditions. For the first time, the effect of BSA on renal and intestinal glucuronidation has been assessed and compared with the effects observed in liver. In vitro data in the presence and absence of BSA were corrected for microsomal recovery to allow assessment of the relative contribution of each tissue to total glucuronidation clearance. These data were then scaled using the well stirred model to assess the impact of BSA on the prediction accuracy of IVIVE of glucuronidation clearance. Prediction accuracy of IVIVE determined using HLM data alone or using combined HLM and HKM data was also investigated.

Materials and Methods

Chemicals. Diclofenac, gemfibrozil, MPA, naloxone, propofol, alamethicin (from *Trichoderma viride*), UDP-glucuronic acid, EDTA, BSA, and saccharic acid lactone were purchased from Sigma-Aldrich (Gillingham, Dorset, UK). Ezetimibe was purchased from Toronto Research Chemicals Inc. (North York, ON, Canada). Telmisartan was purchased from Sequoia Research Products (Pangbourne, UK). All other reagents were of the highest grade available.

Source of the Microsomes. Pooled HLM were purchased from BD Gentest (Woburn, MA). Pooled HKM and HIM were purchased from XenoTech (Tebu-Bio Ltd., Peterborough, Cambridgeshire, UK). Microsomes were stored at −80°C. HLM were pooled from 150 white donors, with 50% female and a mean age of 53 years (range, 18–79 years). HKM were pooled from 8 donors; with 88% white, 50% female, and a mean age of 61 years (range, 48–69 years). HIM were pooled from 18 donors; with 72% white, 39% female, and a mean age of 43 years (range, 21–67 years). Activity for pooled HLM was reported as 0.93, 0.85, 16.0, 2.00, and 0.72 nmol · min^{-1} · mg protein^{-1} for UGT1A1-, UGT1A4-, UGT1A6-, UGT1A9-, and UGT2B7-specific substrates. For HKM and HIM pools, activity was only reported for 4-methylum-

belliferone (a substrate of multiple UGTs); with values of 125 and 8.44 nmol · min^{-1} · mg protein^{-1}, respectively.

Microsome Experimental Conditions. Incubations were performed in duplicate using a Thermomixer (Eppendorf, Hamburg, Germany). The final substrate concentration used was 1 μM, with the exception of propofol for which 5 μM was used. Substrate concentrations were >5-fold below the reported K_m values, when these data were available (Kiang et al., 2005); therefore, the enzyme kinetics assessed are expected to be in the linear range. Microsomal protein concentrations ranged from 0.25 to 1.0 mg/ml; details for individual drugs and tissues are provided in Supplemental Table 1. Microsomes were activated by incubation with alamethicin (50 μg/mg protein) on ice for 15 min (Fisher et al., 2000; Cubitt et al., 2009; Kilford et al., 2009). Substrates were preincubated with activated microsomes and 0.1 M phosphate buffer, pH 7.1, containing 3.45 mM magnesium chloride, 1.15 mM EDTA, and 115 μM saccharic acid lactone, for 5 min at 37°C shaken at 900 rpm (Fisher et al., 2001; Cubitt et al., 2009; Kilford et al., 2009). The reaction was initiated by addition of glucuronic acid (5 mM in incubation) to give a final incubation volume of 1 ml (Cubitt et al., 2009; Kilford et al., 2009). Stability of acyl glucuronides at pH 7.1 was tested using gemfibrozil as a representative example. Gemfibrozil acyl glucuronide was stable at pH 7.1 over the incubation time, and, therefore, this pH was considered to be suitable for microsomal assays of drugs that form this type of glucuronide in the current study. Concentration of the organic solvent used (methanol) was <0.6% of the incubation media. Control incubations were performed for each drug with no cofactor present to account for any potential cofactor-independent loss of the drug over the incubation time. The total length of the incubations ranged from 30 to 60 min (Supplemental Table 1). Samples of 60 to 100 μl of the incubation were removed at each time point and added to an equal volume of ice-cold methanol containing the internal standard as specified in Table 1 to terminate the reaction. Samples were frozen at −20°C for at least 1 h and then thawed and centrifuged (MSE Mistral 3000i centrifuge; MSE, London, UK) at 4°C and 2500 rpm for 30 min. An aliquot of the supernatant (10 or 20 μl) was analyzed by LC-MS/MS for parent drug concentration. Experiments were repeated on three separate occasions with the exception of those with HIM because of limited availability of the microsomal batch investigated.

Incubation conditions for experiments including BSA were comparable to those for experiments without BSA. In preliminary experiments, minimal depletion was observed for the acidic drugs when 2% BSA was used, and, therefore, $CL_{int, UGT}$ could not be determined. This is most likely because acids bind strongly to BSA (Rowland et al., 2009), and the remaining free drug for depletion is minimal. Nonspecific binding of gemfibrozil and diclofenac at BSA concentrations ranging from 0.5 to 2% were determined (data not shown); nonspecific binding was reduced at lower BSA concentrations, but the resultant fraction unbound from protein in the incubation ($f_{u, inc}$) values remained <0.1. Previous research showed a plateau in the increase of $CL_{int, u, UGT}$ results at 1% BSA (Rowland et al., 2007, 2009). Therefore, to allow quantifiable depletion and adequate sequestration of free fatty acids, a concentration of 1% BSA was used for the acidic drugs (diclofenac, gemfibrozil, MPA, and telmisartan), and 2% BSA was found to be suitable for bases/neutral drugs (ezetimibe, naloxone, and propofol). BSA concentration, microsomal protein concentrations, and the total length of the incubations are provided in Supplemental Table 1. The reaction was terminated by adding samples of the incubation to a double volume of ice-cold acetonitrile containing the internal standard. Samples were refrigerated for at least 10 min and then centrifuged (Mini Spin; Eppendorf) at 13,400 rpm and room temperature for 5 min. An aliquot of the supernatant (10 or 20 μl) was analyzed by LC-MS/MS for parent drug concentration. Experiments were repeated 3 times with the exception of those for HIM for which limited availability prevented repeat analysis.

LC-MS/MS. All compounds were analyzed on a Waters 2790 with a Micromass Quattro Ultima triple quadruple mass spectrometer in negative mode with the exception of naloxone and telmisartan, which were analyzed on a Waters 2790 with a Micromass Quattro Micro triple quadruple mass spectrometer in positive mode. Source temperature was 125°C, desolvation temperature was 350°C, desolvation gas rate was 600 l/h, and cone gas rate was 150 l/h, with the exception of MPA and ezetimibe for which cone gas was 50 l/h. The capillary voltage was 3.25 kV for the Micromass Quattro Ultima and 3.5 kV for the Micromass Quattro Micro. Propofol was analyzed using single ion recording owing to its limited fragmentation. Analytes were separated

using a Luna C18 (3 μm, 50 × 4.6 mm) column (Phenomenex, Macclesfield, UK) with the exception of naloxone, for which a Luna Phenyl Hexyl (3 μm, 50 × 4.6 mm) column (Phenomenex) was used. Four mobile phases were used, with varying gradients for each drug: A, 90% water, 10% methanol, and 0.05% formic acid; B, 10% water, 90% methanol, and 0.05% formic acid; C, 90% water, 10% methanol, and 1 mM ammonium acetate; and D, 10% water, 90% methanol, and 1 mM ammonium acetate. The flow rate was 1 ml/min, splitting to 0.25 ml/min before entry into the mass spectrometer. Mass spectrometric conditions for each drug are detailed in Table 1.

Correction for Nonspecific Protein Binding. The high throughput dialysis method (Gertz et al., 2008) was used to determine the $f_{u, inc}$ values for all drugs at 0, 0.1, 0.25, 0.5, and 1.0 mg/ml HLM protein concentrations in the presence and absence of 1 or 2% BSA. Al-Jahdari et al. (2006) reported similar $f_{u, inc}$ values for propofol in HLM and HKM; therefore, nonspecific binding was assumed to be comparable across systems at the same protein concentration. At the low substrate concentrations used herein, nonspecific binding is expected to be below the saturation limit and therefore independent of substrate concentration. This assumption is supported by previous data showing that nonspecific binding of propofol (in the presence and absence of BSA) and MPA (in the absence of BSA) is independent of substrate concentration when determined over a range of concentrations exceeding those used in the current study (Bowalgaha and Miners, 2001; Rowland et al., 2008, 2009). Dialysis membranes (12–14 kDa molecular mass cutoff) were purchased from HTDialysis, LLC (Gales Ferry, CT). Phosphate buffer (0.1 M, pH 7.1), containing 3.45 mM magnesium chloride, 1.15 mM EDTA, 115 μM saccharic acid lactone, and, where applicable, 1 or 2% BSA was added to the acceptor side of the membrane, and the relevant concentration of HLM in buffer was added to the donor side. Each HLM protein concentration was tested in triplicate. A 1 μM concentration of drug (5 μM for propofol) was spiked into each side of the membrane. The plate was left to equilibrate for 6 h on a plate shaker (450 rpm) at 37°C. Then samples from both the acceptor and donor sides of the membrane were transferred to Eppendorf tubes containing an equal volume of methanol with the relevant internal standard for non-BSA samples or a double volume of acetonitrile with internal standard for BSA samples. Sample preparation and LC-MS/MS methods were the same as those for microsomal incubations.

Recovery from equilibrium dialysis was greater than 70% for all drugs with the exception of propofol. Although recovery of propofol was low (<30%), $f_{u, inc}$ values determined both in the presence and absence of BSA were comparable to values reported by Rowland et al. (2008), and so the experimental data have been used. The $f_{u, inc}$ values for the other drugs investigated (both in the presence and absence of BSA) were comparable to values reported in the literature (where available) (Bowalgaha and Miners, 2001; Al-Jahdari et al., 2006; Gertz et al., 2008; Cubitt et al., 2009; Kilford et al., 2009). From preliminary experiments, the volume shift between the donor and acceptor side of the membrane was generally less than 5%, and therefore correction for volume shift had minimal impact on the experimental $f_{u, inc}$.

Nonspecific binding data were analyzed across the range of protein concentrations in GraFit 5 (Erithacus Software, Horley, UK) to determine the binding constant (K_a) for each drug. The K_a was then used to calculate the $f_{u, inc}$ at the protein concentrations used for the glucuronidation depletion assays (eq. 1). The experimentally determined $f_{u, inc}$ values in the presence of BSA were constant over the range of microsomal protein concentrations and, therefore, K_a could not be calculated. In these cases, the mean of the experimental $f_{u, inc}$

values was used for all protein concentrations with BSA. The $CL_{int, UGT}$ values from HLM, HKM, and HIM were corrected for $f_{u, inc}$ ($CL_{int, UGT}/f_{u, inc}$) to generate the unbound intrinsic clearance ($CL_{int, u, UGT}$) (microliters per minute per milligram of protein).

$$f_{u, inc} = \frac{1}{1 + K_a \times C} \tag{1}$$

where C is the microsomal protein concentration.

Data Analysis. The mean concentration of the duplicate samples at each time point was analyzed using GraFit 5 to determine the elimination rate constant (k). A nonlinear single exponential fit was used, with the exception of diclofenac in HLM without BSA for which a double exponential fit was used. The rate constant was used to calculate the $CL_{int, UGT}$ (eq. 2) and corrected for nonspecific binding to give $CL_{int, u, UGT}$ (microliters per minute per milligram of protein).

$$CL_{int, UGT} = \frac{k \times \text{volume of incubation}}{\text{amount of microsomal protein in assay}} \tag{2}$$

To compare $CL_{int, u, UGT}$ values from different tissues, $CL_{int, u, UGT}$ was expressed per gram of tissue by correcting the values for the microsomal protein yield, resulting in scaled $CL_{int, u, UGT}$. Microsomal protein yields of 40, 12.8, and 20.6 mg of protein/g tissue were used for hepatic, renal, and intestinal data, respectively (Al-Jahdari et al., 2006; Barter et al., 2007; Cubitt et al., 2009). In contrast with hepatic microsomal recovery, only one estimate of microsomal recovery for HKMs could be found, based on data from only five donors and an unspecified kidney region (Al-Jahdari et al., 2006). Data from rats support this report; relative microsomal recovery for kidney is 30% of that for liver. The mean scaled $CL_{int, u, UGT}$ and S.D. have been presented for each drug. The mean scaled clearance values were compared using ratios.

Prediction of Intravenous Glucuronidation Clearance. Ezetimibe cannot be dosed intravenously, and the lack of human fraction absorbed and fraction escaping gut metabolism data prevent the conversion of oral plasma clearance data to $CL_{int, UGT}$; therefore, ezetimibe was not included in IVIVE. In vivo pharmacokinetic parameters including intravenous plasma clearance ($CL_{i.v.}$), plasma binding ($f_{u, p}$), blood/plasma ratio (R_B), and renal clearance were collated from the literature for the remaining six drugs. In cases for which multiple clinical studies were available, the mean was calculated, weighted for the number of subjects in each study; references for the in vivo parameters and values from individual studies are shown in Supplemental Tables 2 to 6. Clinical data from Japanese, Korean, and Chinese populations, disease populations, subjects receiving concomitant medication, elderly or obese populations, extended release formulations, and cases in which the area under the curve was reported over an insufficient time period were excluded. No nonlinearity issues were observed across multiple dose levels, so all data were included. Only plasma clearance data were used, with the exception of propofol for which blood data were reported. $CL_{i.v.}$ data for each drug were collated from up to 12 clinical studies (up to 121 subjects in total) (Supplemental Table 2). Data for renal clearance were more limited and for the majority of drugs were available from only one report in the literature. For many of the drugs R_B values were determined in vitro and intersubject variability in this parameter was not assessed. The $f_{u, p}$ data were more readily available in the literature, and values for individual drugs were collated from up to four studies (<59 subjects in total per drug). Intersubject variability for $CL_{i.v.}$ and $f_{u, p}$ was

TABLE 1

LC-MS/MS conditions used for assessing glucuronidation depletion over time of seven drugs in kidney, liver, and intestinal microsomes

Drug	Transition	Cone Voltage	Collision Voltage	Retention Time	Internal Standard	Transition	Cone Voltage	Collision Voltage	Retention Time
		V	*eV*	*min*			*V*	*eV*	*min*
Diclofenac	294.15 > 250.10	30	10	3.50	Tolbutamide	269.00 > 170.00	75	17	2.70
Ezetimibe	408.30 > 271.20	55	15	3.40	Tolbutamide	269.00 > 170.00	75	17	2.80
Gemfibrozil	249.05 > 121.10	67	10	4.45	Tolbutamide	269.00 > 170.00	75	17	2.90
Mycophenolic acid	318.90 > 191.10	90	25	4.40	Warfarin	306.90 > 161.05	130	19	4.60
Naloxone	328.15 > 310.05	30	20	3.30	Levallorphan	284.10 > 156.90	41	45	3.80
Propofol[a]	176.90	60		3.40	Tolbutamide	269.00	75		2.80
Telmisartan	515.00 > 276.00	50	60	3.90	Verapamil	455.10 > 165.00	40	35	3.40

[a] Propofol was measured with single ion recording.

generally <30% within individual studies; values varied to a similar extent between studies, with the exception of $f_{u, p}$ for mycophenolic acid for which values from different studies varied by 48%. The ranges of values from individual studies collated for each parameter are shown elsewhere (Supplemental Tables 2–6).

Plasma $CL_{i.v.}$ of all drugs was corrected for R_B and renal clearance to give blood metabolic clearance (CL_H) (Ito and Houston, 2005; Gertz et al., 2010). Clearance via metabolism was corrected for the fraction metabolized by glucuronidation ($f_{m, UGT}$) to give the apparent in vivo glucuronidation clearance (CL_{UGT}). Where available, data were corrected using in vitro $f_{m, UGT}$ from HLM data in the presence or absence of BSA (from in-house data), which were generated in a pool of HLM with UGT and cytochrome P450 characterization similar to that used for the current work. In the case of MPA and telmisartan, no in vitro $f_{m, UGT}$ data were available; however, for these two drugs in vivo data suggest almost complete glucuronidation ($f_{m, UGT} = 1$ for telmisartan or 0.95 for MPA), and this assumption was applied in IVIVE.

Currently, there are no kidney-specific models available for IVIVE; therefore, perfusion-limited kinetics and assumptions of the well stirred model were applied for the kidney, which may have biased the IVIVE results presented herein. In vitro HLM and HKM $CL_{int, u, UGT}$ data (per gram of tissue) were scaled to give $CL_{int, u, UGT}$ (per kilogram body weight) using average organ weights of 21.4 g of tissue/kg (Ito and Houston, 2005) and 4.5 g tissue/kg for liver and kidney, respectively. The average kidney weight (range from 4.1 to 5.0 g tissue/kg) was estimated from the collated literature reports (Supplemental Table 7). These data were then scaled up using the well stirred model to give apparent glucuronidation clearance for the respective organ (eq. 3) (Houston, 1994). The intestine was expected to have minimal impact on glucuronidation clearance after intravenous drug administration; therefore, HIM $CL_{int, u, UGT}$ data were not included during IVIVE.

$$CL_{UGT} = \frac{CL_{int,u,UGT} \times f_{u,B} \times Q_h}{CL_{int,u,UGT} \times f_{u,B} + Q_h} \quad (3)$$

where $f_{u, B}$ represents fraction unbound in blood, Q_h is hepatic blood flow ($Q_h = 20.7$ ml $\cdot$ min^{-1} $\cdot$ kg^{-1}), and CL_{UGT} represents apparent in vivo glucuronidation clearance. An analogous model was used for the kidney where Q_h was replaced with Q_r (average renal blood flow of 16.4 ml $\cdot$ min^{-1} $\cdot$ kg^{-1}) and in vitro HKM data were used. The values reported for renal blood flow, gender differences, and methods used to estimate this parameters were collated from >50 studies reported in the literature (Supplemental Table 8).

For IVIVE using both the liver and kidney data, combined CL_{UGT} was calculated as the sum of scaled hepatic and renal CL_{UGT}. Predicted CL_{UGT} values from HLM data alone or in combination with HKM data were compared with the observed CL_{UGT} values from in vivo data. Both observed CL_{UGT} and predicted CL_{UGT} values were calculated using $f_{m, UGT}$ and in vitro scaled $CL_{int, u, UGT}$ data determined in the presence of BSA (where available). Similar comparisons were made using data in the absence of BSA. Prediction bias and precision were assessed using geometric fold error and root mean squared error, respectively, as described previously (Gertz et al., 2010).

Results

$CL_{int, UGT}$ was determined for seven drugs in pooled HKM, HLM, and HIM in the presence and absence of BSA using the substrate depletion approach. The $f_{u, inc}$ values were experimentally determined in HLM in the presence and absence of BSA and were used to correct the corresponding $CL_{int, UGT}$ values for nonspecific binding (Table 2).

Glucuronidation Depletion in Human Kidney, Liver, and Intestinal Microsomes in the Absence of Bovine Serum Albumin. Figure 1 illustrates representative examples of depletion rates in different tissues and the effects of BSA on depletion of diclofenac, MPA, and naloxone; individual examples are discussed below in the text. The profiles for the remaining four drugs are shown in Supplemental Fig. 1. Depletion was linear over time for six of the seven drugs; however, for diclofenac a biphasic decline was observed (Fig. 1A). The initial linear decline in diclofenac concentration was used to calculate the $CL_{int, UGT}$. Biphasic depletion of several drugs has been observed both in-house and in literature reports (Cubitt et al., 2009; Kilford et al., 2009) for microsomal and hepatocyte assays (data not shown); however, no trends regarding the assay conditions, type of glucuronide formed (acyl or phenol), substrate physicochemical properties, or UGT specificity could be identified. Reduced microsomal activity over time or end product inhibition may contribute to the observed biphasic decline. Diclofenac assays were performed over 60 min with the initial rate of depletion ending within 10 to 15 min. Assays for other drugs were performed up to 60 min with no apparent decline in depletion rate. Therefore, it is unlikely that the microsomes were losing activity over the incubation. The end of the initial phase occurred after 60 to 80% depletion of diclofenac. For other drugs, no reduction in depletion rate was observed after up to 99% depletion, suggesting that insufficient substrate or cofactor was not the cause of the decrease in diclofenac depletion rate.

For MPA and propofol, the rate of depletion was faster in HKM than in HLM, whereas for diclofenac, ezetimibe, and telmisartan the opposite was observed; for the remaining drugs the depletion rate was similar (Fig. 1, A, C, and E). The rate of depletion in HIM was slower than that in HLM for all drugs and only exceeded that in HKM for ezetimibe and telmisartan (Fig. 1, A, C, and E). The $f_{u, inc}$ in the absence of BSA ranged from 0.18 to 1.00 for ezetimibe and naloxone, respectively and was ≥ 0.65 for six of the seven drugs.

$CL_{int, u, UGT}$ in HKM without BSA ranged from 9.72 to 295 μl $\cdot$ min^{-1} $\cdot$ mg protein^{-1} for telmisartan and ezetimibe, respectively (Table 2). Glucuronidation clearance in HLM without BSA covered a 10-fold larger range than that in HKM ($CL_{int, u, UGT}$ up to 2930 μl $\cdot$ min^{-1} $\cdot$ mg protein^{-1} for ezetimibe). However, the largest range of

TABLE 2

$CL_{int, u, UGT}$ of seven drugs in human kidney, liver, and intestinal microsomes in the presence and absence of bovine serum albumin

Data represent the mean ($\pm$S.D.) of $n = 3$ for human kidney and liver microsomes or $n = 1$ for human intestinal microsomes. Experiments were performed in duplicate.

Drug	$f_{u, inc}$		$CL_{int, u, UGT}$					
			HLM		HKM		HIM	
	− BSA[a]	+ BSA[b]	− BSA	+ BSA	− BSA	+ BSA	− BSA	+ BSA
			$\mu l \cdot min^{-1} \cdot mg\ protein^{-1}$					
Diclofenac	0.98 (0.99, 0.98)	0.02	761 (105)	1190 (195)	177 (57)	543 (90)	74.9	325
Ezetimibe	0.30 (0.18, 0.18)	0.05	2930 (456)	5180 (562)	295 (61)	495 (105)	418	1160
Gemfibrozil	0.90 (0.90, 0.82)	0.01	259 (27)	1840 (312)	265 (6)	1910 (488)	23.9	40.0
Mycophenolic acid	0.83 (0.91, 0.71)	0.18	78.2 (4.6)	233 (44)	293 (58)	1370 (187)	11.8	57.8
Naloxone	1.00 (1.00, 1.00)	0.96	10.0 (1.2)	55.6 (4.1)	10.9 (0.2)	52.7 (6.4)	0.502	14.2
Propofol	0.69 (0.69, 0.69)	0.25	67.8 (4.4)	201 (11.4)	91.5 (31.9)	1023 (130)	62.6	103
Telmisartan	0.65 (0.48, 0.48)	0.07	76.9 (4.2)	395 (57)	9.72 (1.58)	34.3 (17.3)	21.3	91.4

[a] $f_{u, inc}$ at the protein concentration used for depletion assays in HLM (HKM, HIM) (Supplemental Table 1).
[b] One percent BSA used for diclofenac, gemfibrozil, mycophenolic acid, and telmisartan, and 2% BSA used for ezetimibe, naloxone, and propofol.
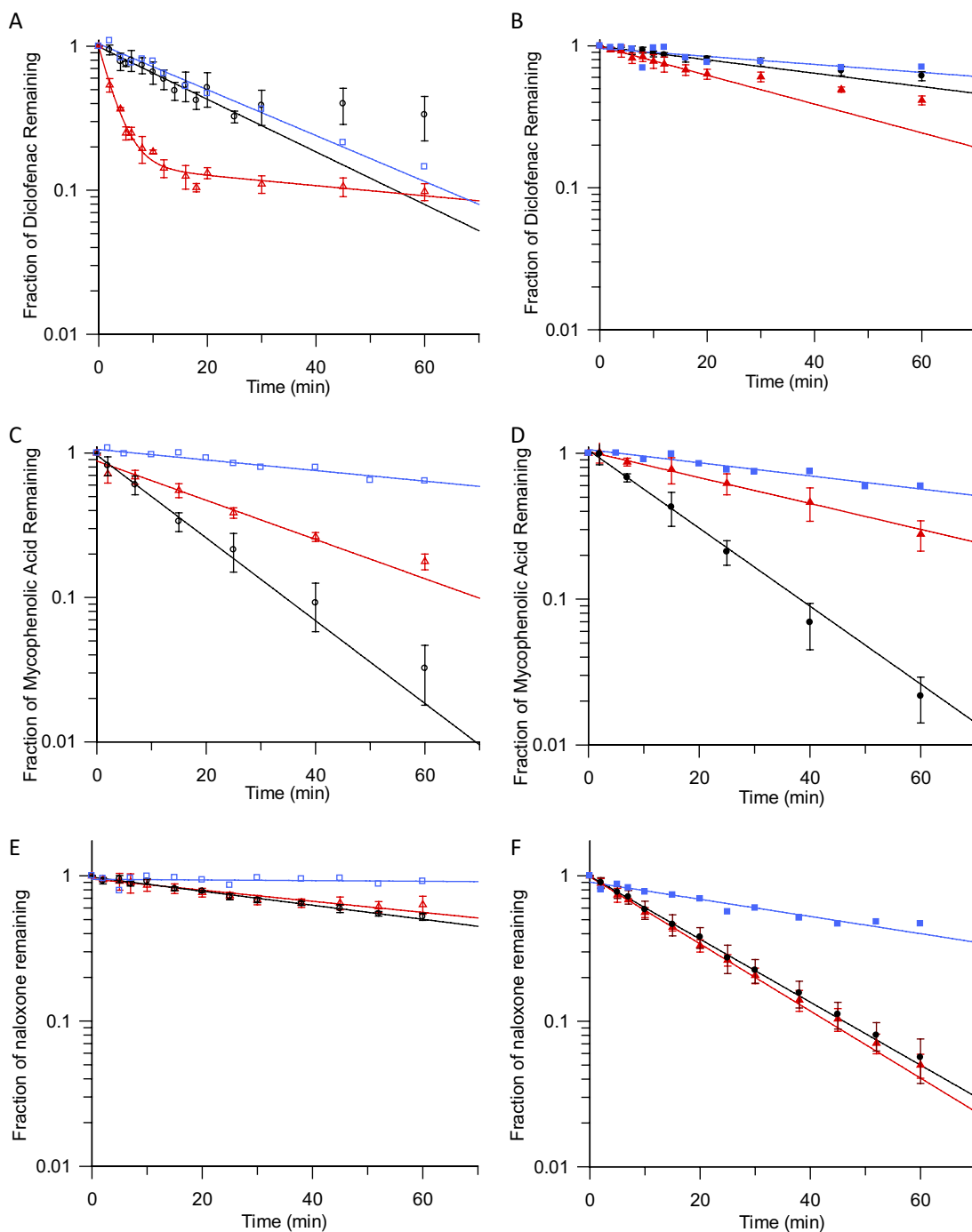
FIG. 1. Mean fraction of drug remaining (±S.D.) over time in human kidney, liver, and intestinal microsomes in the presence (B, D, and F) and absence (A, C, and E) of bovine serum albumin. ○, △, and □, depletion in human kidney, liver, and intestinal microsomes without BSA, respectively; ●, ▲, and ■, depletion in human kidney, liver, and intestinal microsomes with BSA, respectively. A and B, diclofenac. C and D, mycophenolic acid. E and F, naloxone.

$CL_{int, u, UGT}$ for the drugs investigated was observed for HIM (>500-fold), with the lowest value being 0.502 μl · min^{-1} · mg protein^{-1} for naloxone. Ezetimibe had the highest $CL_{int, u, UGT}$ in all tissues, whereas telmisartan or naloxone had the lowest glucuronidation clearance. However, the rank order of clearance values for the other drugs differed among the tissues.

Effect of Albumin on Glucuronidation Depletion by Human Kidney, Liver, and Intestinal Microsomes. All the drugs studied bind strongly to BSA ($f_{u, inc}$ in the presence of BSA = 0.01–0.25) with the exception of naloxone ($f_{u, inc}$ = 0.96) (Table 2); binding to BSA was constant over the 0 to 1 mg/ml HLM protein concentration

range studied. For four of seven drugs investigated, $f_{u, inc}$ under these conditions was <0.1 (Table 2). Because of the reduced free drug available for glucuronidation, the rate of depletion decreased for most drugs upon inclusion of BSA. To allow quantifiable depletion, the microsomal protein concentration in the incubation was increased to 1 mg/ml, and the incubation length was increased to 60 min for diclofenac, gemfibrozil, and telmisartan (Supplemental Table 1). Even with the increase in microsomal protein concentration and incubation length, inclusion of BSA (1% for acids and 2% for bases/neutral drugs) reduced the observed rate of depletion for diclofenac, ezetimibe, and gemfibrozil (Fig. 1, A and B). The biphasic nature of

diclofenac depletion observed without BSA was not apparent in the presence of BSA (Fig. 1, A and B). In contrast, inclusion of BSA increased the rate of depletion for naloxone, MPA, and propofol in HKM (Fig. 1, C–F); these drugs also had the highest $f_{u, inc}$ in the presence of BSA of 0.96, 0.18, and 0.25, respectively. BSA had minimal effect on the rate of depletion for telmisartan or for MPA and propofol in HLM (Fig. 1, C and D). Depletion of telmisartan in HKM in the presence of 1% BSA resulted on average in <10% depletion from the initial concentration over 60 min, most likely as a result of the high binding to BSA, despite the lower BSA concentration used. Depletion from the initial concentration in individual replicates ranged from 0 to 21% at 60 min and also varied by up to 20% at other time points. Clearance estimates for individual incubations of telmisartan in HKM with BSA were consequently highly variable (coefficient of variation = 50%). Data in the absence of BSA showed depletion of 20%, and variability between replicates was low (<20%).

Inclusion of BSA in the incubation resulted in a 56-fold range of renal glucuronidation clearance; telmisartan $CL_{int, u, UGT}$ was the lowest, consistent with the data in the absence of BSA (Table 2). A larger range of $CL_{int, u, UGT}$ was again observed for HLM ($CL_{int, u, UGT}$ up to 5180 $\mu l \cdot min^{-1} \cdot mg\ protein^{-1}$ for ezetimibe) (Table 2). Comparable to HLM, an 82-fold range in $CL_{int, u, UGT}$ was observed for HIM in the presence of BSA. Although the $CL_{int, u, UGT}$ for ezetimibe remained

the highest and that for naloxone remained the lowest in HLM and HIM, the rank order of $CL_{int, u, UGT}$ for the other drugs changed in all tissues after the inclusion of BSA.

Inclusion of BSA increased $CL_{int, u, UGT}$ by 1.6- to 11-fold in all tissues, with the exception of naloxone in the intestine for which $CL_{int, u, UGT}$ increased by 28-fold (Fig. 2). No consistent trends in the increase of $CL_{int, u, UGT}$ resulting from BSA inclusion were observed between the three tissues (Fig. 2). For HLM and HKM, ezetimibe had one of the lowest increases in clearance (1.8- and 1.7-fold, respectively), whereas for HIM similarly low increases in $CL_{int, u, UGT}$ were observed for gemfibrozil and propofol. Similar increases in $CL_{int, u, UGT}$ were observed between HLM and HKM for gemfibrozil and naloxone, whereas the increase in $CL_{int, u, UGT}$ was higher in HKM than in HLM for diclofenac, MPA, and propofol. The increase in intestinal $CL_{int, u, UGT}$ was greater than in liver and kidney for diclofenac, ezetimibe, and naloxone, but lower for gemfibrozil and propofol. The increase in $CL_{int, u, UGT}$ was comparable in HIM and HKM for MPA (4.7- and 4.9-fold, respectively). Upon inclusion of BSA, increases in $CL_{int, u, UGT}$ in this study were generally lower than those reported previously using both the substrate depletion and metabolite formation methods, most noticeably for propofol for which the increases in $CL_{int, u, UGT}$ values were on average 3-fold lower than reported previously (Rowland et al., 2008; Kilford et al., 2009).
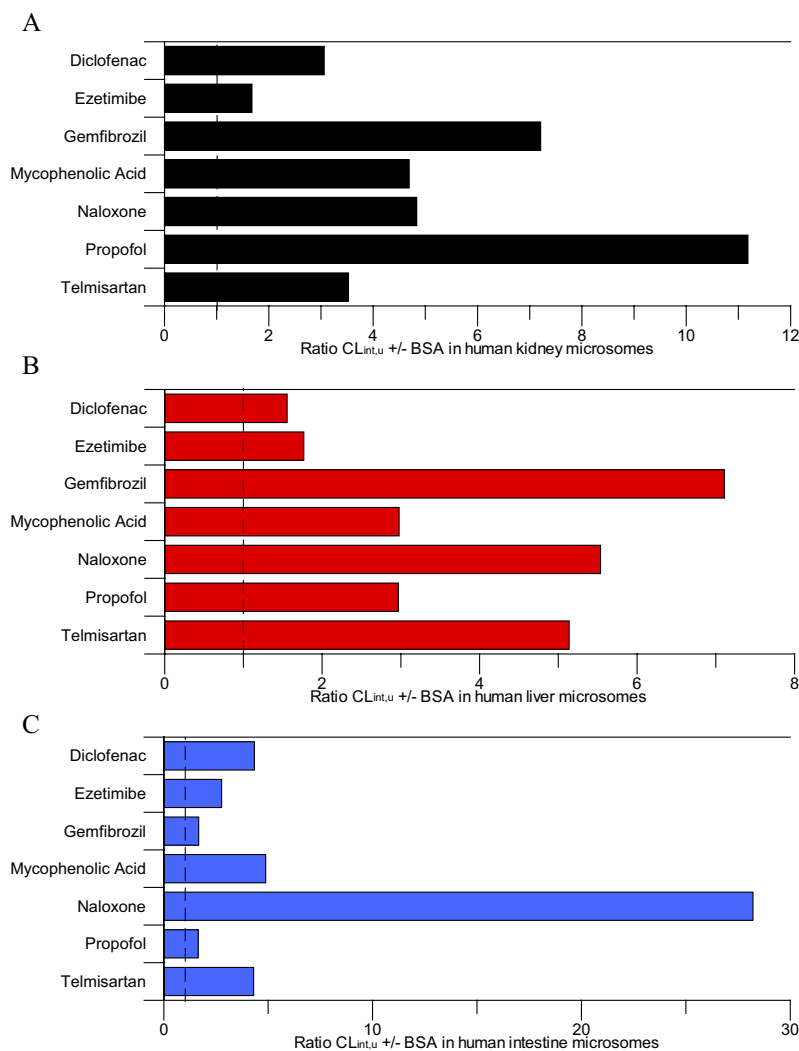

Fig. 2. Ratio of mean glucuronidation $CL_{int, u, UGT}$ $\pm$ bovine serum albumin in human kidney, liver, and intestinal microsomes. A, human kidney microsomes. B, human liver microsomes. C, human intestine microsomes. Dashed line represents the line of unity.

TABLE 3

Scaled $CL_{int, u, UGT}$ of seven drugs from human kidney, liver, and intestinal microsomal data obtained in the absence of albumin

Data represent the mean (±S.D.) of $n = 3$ for human kidney and liver microsomes or $n = 1$ for human intestine microsomes. Experiments were performed in duplicate.

Drug	Primary UGT[a]	$CL_{int, u, UGT}$			Ratio of $CL_{int, u, UGT}$		
		HLM	HKM	HIM	Kidney/Liver	Intestine/Liver	Kidney/Intestine
		ml · min⁻¹ · g tissue⁻¹			*scaled per g tissue*		
Diclofenac	1A9/2B7	30.5 (4.2)	2.27 (0.73)	1.54	0.075	0.051	1.47
Ezetimibe	1A1	117 (18)	3.78 (0.78)	8.61	0.032	0.073	0.439
Gemfibrozil	2B7	10.4 (1.1)	3.39 (0.07)	0.492	0.328	0.048	6.89
Mycophenolic acid	1A9	3.13 (0.18)	3.75 (0.74)	0.244	1.20	0.078	15.4
Naloxone	1A8/2B7	0.402 (0.049)	0.140 (0.003)	0.010	0.348	0.026	13.5
Propofol	1A9	2.71 (0.18)	1.17 (0.41)	1.29	0.432	0.475	0.908
Telmisartan	1A3	3.08 (0.17)	0.124 (0.020)	0.438	0.040	0.142	0.284

[a] References are listed elsewhere (Supplemental Table 10).

Correction of $CL_{int, u, UGT}$ for Microsomal Recovery. In vitro data were corrected for microsomal recovery resulting in scaled $CL_{int, u, UGT}$ values (Tables 3 and 4). After correction, scaled $CL_{int, u, UGT}$ values for HIM without BSA ranged from 0.01 to 8.61 ml · min⁻¹ · g tissue⁻¹ for naloxone and ezetimibe, respectively. Scaled $CL_{int, u, UGT}$ values for HKM without BSA covered a similar range (0.12–3.78 ml · min⁻¹ · g tissue⁻¹ for telmisartan and ezetimibe, respectively). In the absence of BSA, the lowest and highest scaled $CL_{int, u, UGT}$ values for HLM were approximately an order of magnitude greater than those for HIM or HKM (Table 3). In the presence of BSA, the extent of the range of scaled $CL_{int, u, UGT}$ values was similar in all three tissues, but again HLM scaled $CL_{int, u, UGT}$ values were approximately an order of magnitude higher than those obtained in the kidney and intestine (Table 4).

Comparison of In Vitro Glucuronidation Clearance in Kidney Relative to That in Liver. In the absence of BSA, kidney/liver scaled $CL_{int, u, UGT}$ ratios ranged from 0.03 to 1.2 for ezetimibe and MPA, respectively (Table 3). MPA was the only drug for which scaled $CL_{int, u, UGT}$ values obtained in the absence of BSA were greater in kidney than in liver microsomes (Fig. 3A). Scaled glucuronidation clearance by kidney microsomes represented 32 to 43% of that in liver for gemfibrozil, naloxone, and propofol and for the remaining drugs the renal scaled $CL_{int, u, UGT}$ was <8% of that in the liver (Fig. 3A). Inclusion of BSA gave a similar range of kidney/liver ratios (Table 4); however, in addition to MPA, scaled $CL_{int, u, UGT}$ for propofol was higher in the kidney than in the liver (Fig. 3B). Comparison of kidney and liver scaled $CL_{int, u, UGT}$ values remained similar for the other drugs after addition of BSA (Table 4). No trends between the scaled $CL_{int, u, UGT}$ values in liver and the ratio of kidney/liver scaled clearance were observed.

Comparison of In Vitro Glucuronidation Clearance in Intestine Relative to That in Liver. Intestinal scaled $CL_{int, u, UGT}$ in the ab-

sence of BSA represented <15% of that in the liver for all drugs, with the exception of propofol for which the intestinal scaled $CL_{int, u, UGT}$ was 48% of that in the liver (Fig. 3C). Addition of BSA increased intestine/liver scaled clearance ratios by approximately 2-fold for four of seven drugs. In the case of telmisartan, the clearance ratio between intestine and liver remained unchanged, whereas it decreased for propofol and gemfibrozil, in the latter case to 1% of the liver (Fig. 3D). Analogous to renal glucuronidation, no trends between the scaled clearance in liver and the intestine/liver scaled $CL_{int, u, UGT}$ ratios were observed.

Comparison of In Vitro Glucuronidation Clearance in Kidney Relative to That in Intestine. Scaled $CL_{int, u, UGT}$ without BSA was higher in the kidney than in the intestine for diclofenac, gemfibrozil, MPA, and naloxone (kidney/intestine ratios = 1.47–15.4). For the remaining three drugs, scaled clearance by the kidney represented 28 to 91% of that in the intestine. There were no consistent trends in the change in kidney/intestine ratios upon inclusion of BSA. Scaled $CL_{int, u, UGT}$ was higher in the kidney than that in the intestine for five of seven drugs in the presence of BSA with kidney/intestine scaled $CL_{int, u, UGT}$ ratios ranging from 0.23 to 29.7 for telmisartan and gemfibrozil, respectively (Table 4).

Prediction of Intravenous Glucuronidation Clearance. In vitro hepatic and renal scaled $CL_{int, u, UGT}$ values for six drugs were further scaled up using the well stirred model and compared with observed in vivo intravenous CL_{UGT}. Table 5 provides a summary of the in vivo and in vitro data used for IVIVE; full details of the in vivo parameters are presented elsewhere (Supplemental Tables 2–6). Prediction success for IVIVE of scaled $CL_{int, u, UGT}$ using HLM data alone or in combination with HKM data is shown in Fig. 4 (full details in Supplemental Table 9). Comparison of predicted to observed intravenous CL_{UGT} from HLM data alone in the presence of BSA leads to a median underprediction of 66% with diclofenac, MPA, and naloxone

TABLE 4

Scaled $CL_{int, u, UGT}$ of seven drugs from human kidney, liver, and intestinal microsomal data obtained in the presence of 1 or 2% bovine serum albumin

Data represent the mean (±S.D.) of $n = 3$ for human kidney and liver microsomes or $n = 1$ for human intestine microsomes. Experiments were performed in duplicate.

Drug[a]	Primary UGT[b]	$CL_{int, u, UGT}$			Ratio of $CL_{int, u, UGT}$		
		HLM	HKM	HIM	Kidney/Liver	Intestine/Liver	Kidney/Intestine
		ml · min⁻¹ · g tissue⁻¹			*scaled per g tissue*		
Diclofenac	1A9/2B7	47.4 (7.8)	6.95 (1.15)	6.70	0.147	0.141	1.04
Ezetimibe	1A1	207 (23)	6.34 (1.34)	23.8	0.031	0.115	0.266
Gemfibrozil	2B7	73.6 (12.5)	24.4 (6.2)	0.824	0.332	0.011	29.7
Mycophenolic Acid	1A9	9.32 (1.77)	17.6 (2.4)	1.19	1.89	0.128	14.8
Naloxone	1A8/2B7	2.22 (0.17)	0.675 (0.082)	0.292	0.304	0.131	2.31
Propofol	1A9	8.05 (0.46)	13.1 (1.66)	2.13	1.63	0.264	6.16
Telmisartan	1A3	15.8 (2.3)	0.439 (0.222)	1.88	0.028	0.119	0.233

[a] One percent BSA used for diclofenac, gemfibrozil, mycophenolic acid, and telmisartan, and 2% BSA used for ezetimibe, naloxone, and propofol.
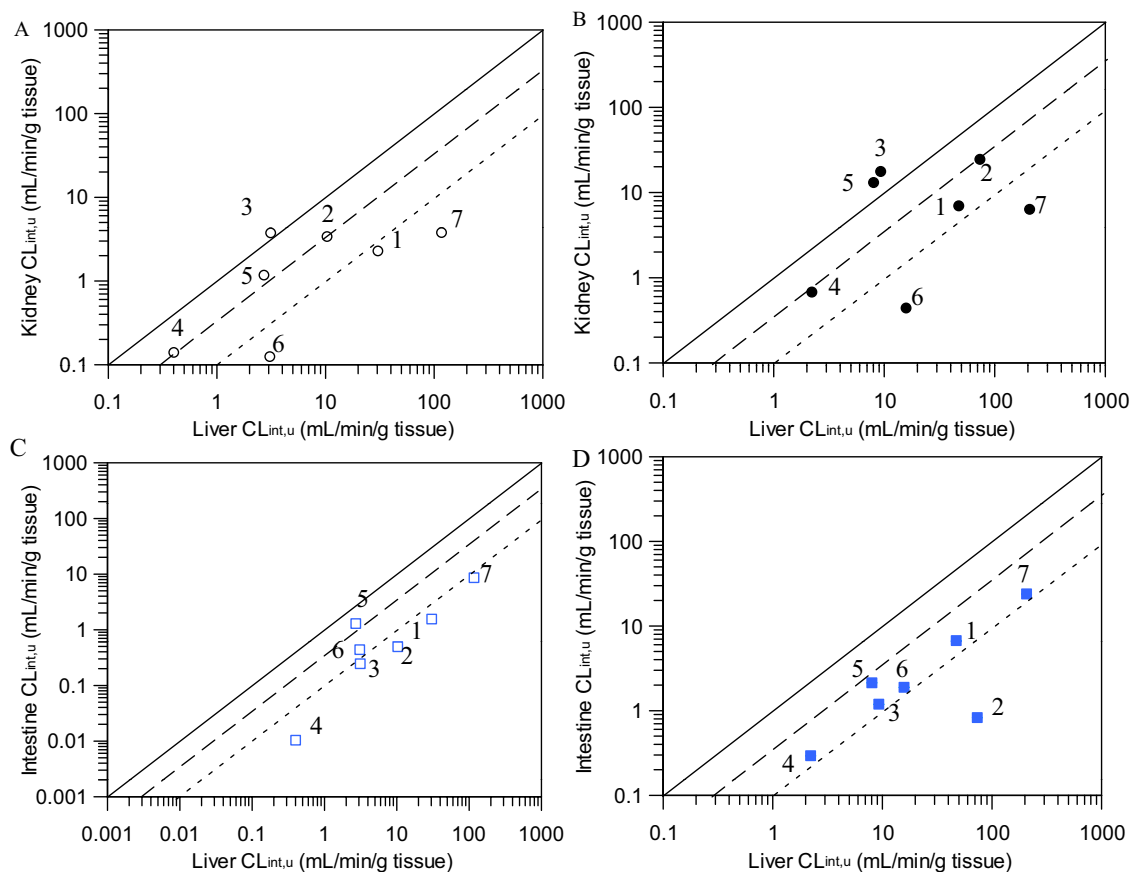[b] References are listed elsewhere (Supplemental Table 10).

FIG. 3. Comparison of mean scaled $CL_{int, u, UGT}$ in human kidney and intestinal microsomes compared with liver scaled $CL_{int, u, UGT}$ in the presence and absence of bovine serum albumin. A and B, represent kidney versus liver scaled $CL_{int, u, UGT}$. C and D, represent intestine versus liver scaled $CL_{int, u, UGT}$. ○ and □, represent $CL_{int, u, UGT}$ data obtained in the absence of BSA; ● and ■, represent $CL_{int, u, UGT}$ data generated in the presence of BSA. ——, line of unity; – – –, 3-fold difference; - - -, 10-fold difference. 1, diclofenac; 2, gemfibrozil; 3, mycophenolic acid; 4, naloxone; 5, propofol; 6, telmisartan; 7, ezetimibe.

being predicted within 2-fold of observed values (Fig. 4A). A 3-fold prediction bias was observed and precision (root mean squared error) was 6.60. Predicted clearance ranged from 13 to 102% of observed values for telmisartan and diclofenac, respectively, with the exception of gemfibrozil for which predicted CL_{UGT} was 3.6-fold greater than the observed value. Use of hepatic microsomal data obtained in the absence of BSA resulted in reduced prediction success for most of the drugs investigated, with increased bias (15-fold) and only two of six drugs predicted within 2-fold of the observed CL_{UGT}. The exceptions were propofol and gemfibrozil for which predicted clearance based on the data in the absence of BSA was in better agreement with observed values (Fig. 4). Predictions from HLM data alone in the absence of BSA performed slightly better than those reported previously; the mean predicted CL_{UGT} was 39% of observed CL_{UGT} versus 10 to 22% in previous reports (Soars et al., 2002; Cubitt et al., 2009; Kilford et al., 2009).

Upon inclusion of renal CL_{UGT} (in the presence of BSA) predictions of MPA, naloxone, and propofol were all improved compared with use of HLM data alone (percentage of predicted/observed CL_{UGT} increased from 72 to 102, from 61 to 69, and from 18 to 24%, respectively) (Fig. 4B). However, a comparable increase in the overprediction of gemfibrozil CL_{UGT} was observed, and therefore the overall prediction success remained similar to using HLM data alone. In the absence of BSA, inclusion of renal CL_{UGT} showed marginal improvement in prediction accuracy compared with predictions based on HLM data in isolation (Fig. 4B). Soars et al. (2002) reported a more pronounced increase in prediction accuracy when scaled renal $CL_{int, u, UGT}$ (in the absence of BSA) was

included in IVIVE. However, kidney and liver microsomal protein recoveries were assumed to be equivalent in Soars et al. (2002), in contrast to the current study in which lower protein recovery for kidney relative to liver was applied, leading to a potentially underestimated impact of renal glucuronidation.

Diclofenac, gemfibrozil, and telmisartan all had very low $f_{u, inc}$ in the presence of BSA (<0.07), and any errors associated with experimental determination may have a pronounced effect on the success of CL_{UGT} prediction. However, the $f_{u, inc}$ value for gemfibrozil and telmisartan would have to differ substantially (up to 7-fold) for the predicted clearance to be within 2-fold of observed values. The $f_{u, inc}$ value for diclofenac in the presence of BSA was also in this range (<0.1), but its CL_{UGT} was predicted well. In addition, all nonspecific binding experiments were conducted at five microsomal concentrations (three replicates of each). For gemfibrozil and telmisartan, recovery was high (88–100%), and low variability between the $f_{u, inc}$ values of individual replicates (coefficient of variation of 11 and 14%, respectively) was observed. It is therefore unlikely that nonspecific binding or any errors associated with low $f_{u, inc}$ estimates can in isolation rationalize the pronounced over/underpredictions of CL_{UGT} for gemfibrozil and telmisartan. For many of the drugs studied, $f_{u, p}$ values were also very low (<0.02 for five of the six drugs), and the variability associated with this parameter was generally <30% for individual drugs in the data set (Supplemental Table 4). Varying $f_{u, p}$ values by this magnitude had a marginal impact on the prediction accuracy of IVIVE and could not in isolation rationalize the pronounced over/underpredictions of CL_{UGT} for gemfibrozil, naloxone, propofol, and telmisartan.

TABLE 5

In vitro and in vivo parameters used for IVIVE of glucuronidation clearance in human liver and kidney microsomes in the absence and presence of 1 or 2% bovine serum albumin

In vivo parameter data represent weighted mean; details of variability between literature reports are given elsewhere (Supplemental Tables 2–6). Predicted CL_{UGT} data represent the mean ($\pm$S.D.) of $n = 3$ for human kidney and liver microsomes.

Drug	In Vivo Parameters[a]				$f_{m, UGT}$[b]		Observed CL_{UGT}		Derived Parameters			
									Predicted CL_{UGT}			
									HLM Only		HLM + HKM	
	$CL^{i.v.}$	Renal CL	fu, p	R_B	− BSA	+ BSA	− BSA	+ BSA	− BSA	+ BSA	− BSA	+ BSA
	$ml \cdot min^{-1} \cdot kg^{-1}$						$ml \cdot min^{-1} \cdot kg^{-1}$		$ml \cdot min^{-1} \cdot kg^{-1}$			
Diclofenac	4.84	0.06	0.004	0.71[c]	0.62	0.65	4.19	4.40	3.12 (0.49)	4.48 (0.90)	3.18 (0.51)	4.65 (0.93)
Gemfibrozil	1.70	0.02	0.005[c]	0.75[c]	0.79	0.86	1.78	1.93	1.38 (0.15)	6.97 (1.64)	1.48 (0.16)	7.67 (1.83)
Mycophenolic acid	2.49	0.01	0.010	0.60	0.95[d]	0.95[d]	3.97	3.97	1.05 (0.06)	2.84 (0.61)	1.33 (0.12)	4.06 (0.78)
Naloxone	21.70	0.00	0.570	1.00[e]	0.65	0.89	14.1	19.3	3.96 (0.59)	11.7 (1.83)	4.31 (0.59)	13.3 (2.04)
Propofol	27.72[f]	0.00	0.015	0.88	0.14	0.53	3.88	14.7	0.959 (0.065)	2.61 (0.17)	1.05 (0.10)	3.57 (0.30)
Telmisartan	12.32	0.00	0.005	1.24[c]	1.00[d]	1.00[d]	9.93	9.93	0.262 (0.014)	1.28 (0.20)	0.264 (0.015)	1.29 (0.20)

[a] References are listed elsewhere (Supplemental Tables 2–6).
[b] $f_{m, UGT}$ values taken from in-house data were available.
[c] Measurement made in vitro.
[d] No suitable in vitro data were available so in vivo $f_{m, UGT}$ was used.
[e] No data available; value of 1 assumed for basic drugs.
[f] Blood clearance data.

Discussion

This study characterized and compared extrahepatic and hepatic glucuronidation in alamethicin-activated microsomes for diclofenac, ezetimibe, gemfibrozil, MPA, naloxone, propofol, and telmisartan using standardized assay conditions. The impact of BSA on microsomal assays has previously been investigated for hepatic glucuronidation (Rowland et al., 2008; Kilford et al., 2009), and its effects on extrahepatic glucuronidation are reported here. The impact of albumin on the relative ratios in $CL_{int, u, UGT}$ among tissues was investigated. IVIVE including both kidney and liver $CL_{int, u, UGT}$ was performed, and the impact of BSA on prediction accuracy was assessed.

Impact of BSA on Microsomal Glucuronidation Clearance in Three Tissues. Inclusion of BSA in HLM incubations increased $CL_{int, u, UGT}$ up to 7-fold, which is within the range of previously reported data (Kilford et al., 2009; Rowland et al., 2009; Manevski et al., 2011). In addition, the presence of BSA in the incubations led to increases in HKM and HIM $CL_{int, u, UGT}$ values, supporting reports that linoleic and arachidonic acids (the most potent UGT inhibitors of FFAs) (Tsoutsikos

et al., 2004) are abundant in all three tissues investigated (Soydan et al., 1996; Hoffmann et al., 2005; Rowland et al., 2007). Inclusion of BSA (1% for acids and 2% for bases/neutral drugs) decreased the $f_{u, inc}$ for all drugs (<0.1 for four of seven drugs); consequently, depletion was very low for some of the drugs investigated. For highly bound drugs, the accuracy of $f_{u, inc}$ may have a significant impact on $CL_{int, u, UGT}$ values and subsequent IVIVE. Consideration of alternatives (e.g., human intestinal fatty acid binding protein with reduced drug binding) as proposed by Rowland et al. (2009) might eliminate some of these issues, but unfortunately this protein was not available at the time of the current study.

In HLM, drugs cleared primarily by UGT1A9 and UGT2B7 showed similar increases in $CL_{int, u, UGT}$ upon inclusion of BSA. Ezetimibe is mainly cleared via UGT1A1 and had the smallest increase in HLM and HKM $CL_{int, u, UGT}$ in the presence of BSA. UGT1A9 substrates (propofol and MPA) showed a more pronounced increase in $CL_{int, u, UGT}$ in HKM than in HLM, which could potentially be attributed to higher expression of UGT1A9 in kidney tissue. Surprisingly, diclofenac (primarily cleared via UGT2B7) showed a low increase in HLM $CL_{int, u, UGT}$; as described
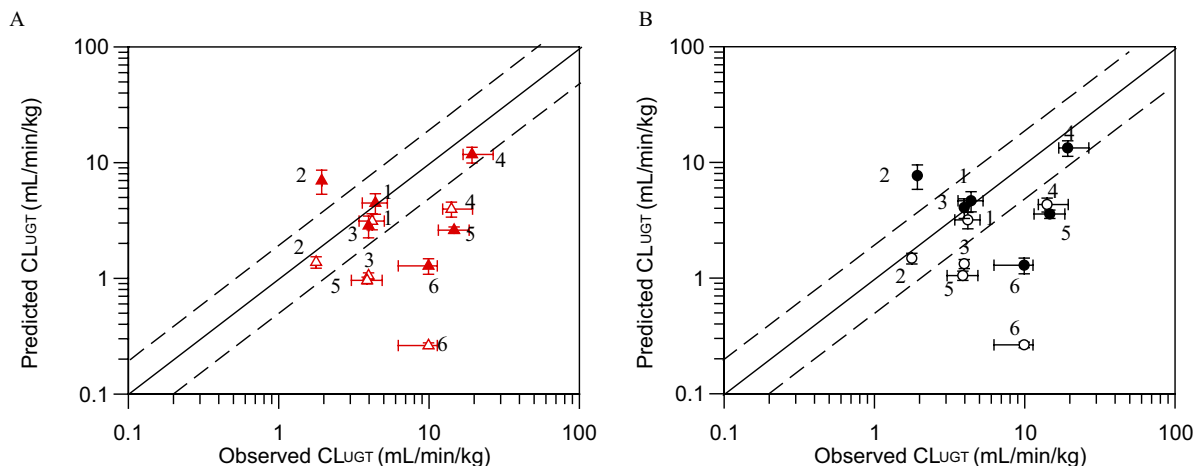

FIG. 4. Comparison of observed intravenous to predicted CL_{UGT} calculated using the well stirred model and mean ($n = 3$) in vitro human liver microsomal (A) or combined human liver and kidney microsomal (B) data in the presence and absence of bovine serum albumin. Observed intravenous clearance data were corrected for R_B, renal clearance, and $f_{m, UGT}$. $\triangle$ and $\blacktriangle$, human liver microsome data only; $\bigcirc$ and $\bullet$, combined human liver and kidney microsomal data. $\triangle$ and $\bigcirc$, data obtained in the absence of BSA; $\blacktriangle$ and $\bullet$, data obtained in the presence of BSA. ——, line of unity; – – –, 2-fold difference. Vertical bars represent S.D. for in vitro data; horizontal bars represent minimum and maximum in vivo CL_{UGT} values (calculated from minimum and maximum $CL_{i.v.}$ values; Supplemental Table 2). 1, diclofenac; 2, gemfibrozil; 3, mycophenolic acid; 4, naloxone; 5, propofol; 6, telmisartan.

above, this increase was less pronounced than that for HKM $CL_{int, u, UGT}$. Gemfibrozil and naloxone had comparable increases in $CL_{int, u, UGT}$ in kidney and liver, indicating similar effects of BSA on UGT2B7 in these tissues. Trends observed in HLM and HKM are in agreement with limited available UGT mRNA/protein expression data, indicating higher expression of UGT1A9 in the kidney and comparable UGT2B7 expression in kidney and liver (Nishimura and Naito, 2006; Ohno and Nakajin, 2009; Harbourt et al., 2012; Ohtsuki et al., 2012). Lower expression of these UGTs reported in the intestine is in contrast to the pronounced increases in $CL_{int, u, UGT}$ observed for diclofenac, ezetimibe, and naloxone in intestinal microsomes upon inclusion of BSA.

Telmisartan is minimally cleared via UGT1A9 but showed one of the largest increases in $CL_{int, u, UGT}$ in HLM and HIM. This result may suggest that other UGTs involved in its clearance (UGT1A3 > 1A1/1A7/1A8) may also be affected by FFAs. Arachidonic acid is cleared via UGT1A3 (Little et al., 2004) and, therefore, may cause competitive inhibition of this enzyme, which would rationalize the large increase in $CL_{int, u, UGT}$ observed for telmisartan. Gemfibrozil is also partially cleared via UGT1A3 and showed >6-fold increases in clearance in HLM and HKM. For naloxone (UGT1A8 and UGT2B7 substrate), $CL_{int, u, UGT}$ increased by 28-fold in HIM in the presence of albumin, whereas the increase in gemfibrozil $CL_{int, u, UGT}$ (mainly UGT2B7 substrate) was only 2-fold. These findings suggest that UGT1A8 may also be inhibited by FFAs; to date, the effect of FFAs and BSA on UGT1A3 and the intestinal specific UGTs has not been studied. The effect of BSA on the different tissues may also be influenced by differences in their FFA content.

Comparison of In Vitro Glucuronidation Clearance in Different Tissues. Inclusion of BSA altered the ratios of scaled clearance between different tissues in a substrate-dependent manner. Scaled renal $CL_{int, u, UGT}$ (per gram of tissue) obtained in the presence of BSA was 3% of that in liver for substrates cleared primarily by UGT1A1 and UGT1A3 (ezetimibe and telmisartan). In contrast, for UGT1A9 substrates (propofol and MPA), scaled renal $CL_{int, u, UGT}$ was up to 2-fold higher than hepatic values, suggesting that expression of UGT1A1 and UGT1A3 is lower and that of UGT1A9 is higher in the kidney than in the liver. The kidney/liver scaled $CL_{int, UGT}$ ratios for drugs primarily cleared by UGT2B7 ranged from 0.15 to 0.33, potentially because of lower expression of UGT2B7 in the kidney than in the liver or higher expression of other contributing UGTs for these drugs in the liver.

Our data showed the highest intestine/liver ratio for propofol. If propofol is selectively glucuronidated by UGT1A9, the tissue ratios should not change after inclusion of BSA; however, this was not the case, indicating that propofol may also be cleared by other UGTs, in agreement with previous reports that UGT1A8 contributes to propofol glucuronidation (Cheng et al., 1999). For the drugs predominantly cleared by UGT1A1 and UGT1A3, the intestine/liver $CL_{int, u, UGT}$ ratios were low. The scaled renal $CL_{int, u, UGT}$ was lower than that in intestine for these drugs, suggesting that UGT1A1 and UGT1A3 are most highly expressed in liver followed by intestine. These functional activity data are compatible with currently available UGT mRNA/protein expression data (Nishimura and Naito, 2006; Ohno and Nakajin, 2009; Harbourt et al., 2012; Ohtsuki et al., 2012).

For non-BSA data, the kidney/liver scaled $CL_{int, u, UGT}$ ratios were generally lower than those calculated from previously published data, with the exception of MPA (Bowalgaha and Miners, 2001; Shipkova et al., 2001; Bernard and Guillemette, 2004). Intestine/liver scaled $CL_{int, u, UGT}$ ratios for diclofenac, gemfibrozil, and naloxone were also lower than those calculated from data in Cubitt et al. (2009), with the exception of propofol (Raoof et al., 1996). Differences in the tissue scaled $CL_{int, u, UGT}$ ratios between studies could arise from the use of microsomes from different donors (Court, 2010), use of microsomes prepared from different sections of the kidney or intestine (generally not reported), inconsistencies in assay conditions and scaling factors applied.

Prediction of Intravenous Glucuronidation Clearance. Prediction of intravenous CL_{UGT} from HLM data alone in the presence of BSA resulted in underestimation of in vivo clearance, with three of the six drugs predicted within 2-fold of observed values. Similar to data reported by Kilford et al. (2009), gemfibrozil CL_{UGT} was overpredicted. In agreement with previous reports, IVIVE of in vitro data in the absence of BSA resulted in reduced prediction success for most of the drugs investigated (Rowland et al., 2007, 2008, 2009; Kilford et al., 2009).

Inclusion of renal CL_{UGT} increased prediction success for several drugs with half of the drugs being predicted well. The largest impact was observed for MPA and propofol, which is not surprising, considering that these drugs had a higher scaled renal $CL_{int, u, UGT}$ than liver $CL_{int, u, UGT}$. However, inclusion of renal CL_{UGT} also increased the overprediction observed for gemfibrozil. Further analysis of a larger set of drugs and development of more physiologically based kidney models will allow more conclusive assessment of the impact of renal CL_{UGT} in IVIVE. Robust scaling factors for extrahepatic glucuronidation are yet to be substantiated, and interpretation of $CL_{int, UGT}$ differences between tissues is problematic. Scaling of $CL_{int, u, UGT}$ values using absolute abundance of individual UGTs may alter the tissue $CL_{int, u, UGT}$ ratios reported here. Abundance data from a large cohort of individuals (as in the case of cytochromes P450), information on regional expression differences across tissues of interest, and appropriate covariate analysis are required to allow further refinement of IVIVE of glucuronidation clearance and associated variability.

Errors in the accuracy of plasma or nonspecific binding estimates in isolation could not explain the poor predictions for gemfibrozil, propofol, naloxone, and telmisartan. However, variability in $f_{u, p}$ or other pharmacokinetic parameters collated from the literature combined with any errors in $f_{u, inc}$ estimation may have contributed to the poor IVIVE accuracy observed for some drugs. In addition, renal $CL_{int, u, UGT}$ was determined from a very limited pool of donors in comparison with liver $CL_{int, u, UGT}$, and, therefore, any variability due to the age and/or health of these donors could not be accounted for in IVIVE. Use of more dynamic modeling techniques, e.g., physiologically based pharmacokinetic models, may improve predictions of CL_{UGT} for drugs such as telmisartan, for which transporters play an important role in drug disposition (Ishiguro et al., 2006; Menochet et al., 2011). For nontransporter substrates, the use of physiologically based models may provide limited improvement as issues associated with the UGT scaling factors will affect their prediction accuracy, analogous to the current IVIVE strategy.

In conclusion, this is the first publication assessing the effect of BSA on characterization and comparison of glucuronidation in kidney, intestine, and liver. Use of 1% BSA for acids and 2% for bases/neutral drugs was found to be suitable for determination of $CL_{int, UGT}$ in microsomes from all three tissues. Inclusion of BSA in microsomal glucuronidation assays increased $CL_{int, u, UGT}$ in a tissue- and drug-dependent manner, altered the ratios of clearance between the tissues, and resulted in improved overall prediction accuracy of clearance. The potential for intestinal specific UGTs and UGT1A3 to be inhibited by FFAs, highlighted by the current findings, requires further investigation. For four of the seven drugs, the scaled renal $CL_{int, u, UGT}$ (with BSA) represented >30% of that in the liver, being higher than that in the liver for UGT1A9 substrates. Inclusion of renal CL_{UGT} in IVIVE further improved predictions for some drugs, most noticeably for substrates of UGT1A9, and, therefore, should be characterized in the future for drugs cleared by this enzyme.

Authorship Contributions

Participated in research design: Gill, Houston, and Galetin.
Conducted experiments: Gill.
Performed data analysis: Gill.
Wrote or contributed to the writing of the manuscript: Gill, Houston, and Galetin.

References

Al-Jahdari WS, Yamamoto K, Hiraoka H, Nakamura K, Goto F, and Horiuchi R (2006) Prediction of total propofol clearance based on enzyme activities in microsomes from human kidney and liver. *Eur J Clin Pharmacol* **62:**527–533.

Barter ZE, Bayliss MK, Beaune PH, Boobis AR, Carlile DJ, Edwards RJ, Houston JB, Lake BG, Lipscomb JC, Pelkonen OR, et al. (2007) Scaling factors for the extrapolation of in vivo metabolic drug clearance from in vitro data: reaching a consensus on values of human microsomal protein and hepatocellularity per gram of liver. *Curr Drug Metab* **8:**33–45.

Bellemare J, Rouleau M, Harvey M, Popa I, Pelletier G, Têtu B, and Guillemette C (2011) Immunohistochemical expression of conjugating UGT1A-derived isoforms in normal and tumoral drug-metabolizing tissues in humans. *J Pathol* **223:**425–435.

Bernard O and Guillemette C (2004) The main role of UGT1A9 in the hepatic metabolism of mycophenolic acid and the effects of naturally occurring variants. *Drug Metab Dispos* **32:**775–778.

Boase S and Miners JO (2002) In vitro-in vivo correlations for drugs eliminated by glucuronidation: investigations with the model substrate zidovudine. *Br J Clin Pharmacol* **54:**493–503.

Bowalgaha K and Miners JO (2001) The glucuronidation of mycophenolic acid by human liver, kidney and jejunum microsomes. *Br J Clin Pharmacol* **52:**605–609.

Cheng Z, Radominska-Pandya A, and Tephly TR (1999) Studies on the substrate specificity of human intestinal UDP-glucuronosyltransferases 1A8 and 1A10. *Drug Metab Dispos* **27:**1165–1170.

Court MH (2010) Interindividual variability in hepatic drug glucuronidation: studies into the role of age, sex, enzyme inducers, and genetic polymorphism using the human liver bank as a model system. *Drug Metab Rev* **42:**209–224.

Cubitt HE, Houston JB, and Galetin A (2009) Relative importance of intestinal and hepatic glucuronidation—impact on the prediction of drug clearance. *Pharm Res* **26:**1073–1083.

Fisher MB, Campanale K, Ackermann BL, VandenBranden M, and Wrighton SA (2000) In vitro glucuronidation using human liver microsomes and the pore-forming peptide alamethicin. *Drug Metab Dispos* **28:**560–566.

Fisher MB, Paine MF, Strelevitz TJ, and Wrighton SA (2001) The role of hepatic and extrahepatic UDP-glucuronosyltransferases in human drug metabolism. *Drug Metab Rev* **33:**273–297.

Gaganis P, Miners JO, Brennan JS, Thomas A, and Knights KM (2007) Human renal cortical and medullary UDP-glucuronosyltransferases (UGTs): immunohistochemical localization of UGT2B7 and UGT1A enzymes and kinetic characterization of *S*-naproxen glucuronidation. *J Pharmacol Exp Ther* **323:**422–430.

Gertz M, Harrison A, Houston JB, and Galetin A (2010) Prediction of human intestinal first-pass metabolism of 25 CYP3A substrates from in vitro clearance and permeability data. *Drug Metab Dispos* **38:**1147–1158.

Gertz M, Kilford PJ, Houston JB, and Galetin A (2008) Drug lipophilicity and microsomal protein concentration as determinants in the prediction of the fraction unbound in microsomal incubations. *Drug Metab Dispos* **36:**535–542.

Hallifax D, Foster JA, and Houston JB (2010) Prediction of human metabolic clearance from in vitro systems: retrospective analysis and prospective view. *Pharm Res* **27:**2150–2161.

Harbourt DE, Fallon JK, Ito S, Baba T, Ritter JK, Glish GL, and Smith PC (2012) Quantification of human uridine-diphosphate glucuronosyl transferase 1A isoforms in liver, intestine, and kidney using nanobore liquid chromatography-tandem mass spectrometry. *Anal Chem* **84:**98–105.

Hoffmann K, Blaudszun J, Brunken C, Höpker WW, Tauber R, and Steinhart H (2005) New application of a subcellular fractionation method to kidney and testis for the determination of conjugated linoleic acid in selected cell organelles of healthy and cancerous human tissues. *Anal Bioanal Chem* **381:**1138–1144.

Houston JB (1994) Utility of in vitro drug metabolism data in predicting in vivo metabolic clearance. *Biochem Pharmacol* **47:**1469–1479.

Ishiguro N, Maeda K, Kishimoto W, Saito A, Harada A, Ebner T, Roth W, Igarashi T, and Sugiyama Y (2006) Predominant contribution of OATP1B3 to the hepatic uptake of telmisartan, an angiotensin II receptor antagonist, in humans. *Drug Metab Dispos* **34:**1109–1115.

Ito K and Houston JB (2005) Prediction of human drug clearance from in vitro and preclinical data using physiologically based and empirical approaches. *Pharm Res* **22:**103–112.

Izukawa T, Nakajima M, Fujiwara R, Yamanaka H, Fukami T, Takamiya M, Aoki Y, Ikushiro S, Sakaki T, and Yokoi T (2009) Quantitative analysis of UDP-glucuronosyltransferase (UGT) 1A and UGT2B expression levels in human livers. *Drug Metab Dispos* **37:**1759–1768.

Kiang TK, Ensom MH, and Chang TK (2005) UDP-glucuronosyltransferases and clinical drug-drug interactions. *Pharmacol Ther* **106:**97–132.

Kilford PJ, Stringer R, Sohal B, Houston JB, and Galetin A (2009) Prediction of drug clearance by glucuronidation from in vitro data: use of combined cytochrome P450 and UDP-glucuronosyltransferase cofactors in alamethicin-activated human liver microsomes. *Drug Metab Dispos* **37:**82–89.

Knights KM, Winner LK, Elliot DJ, Bowalgaha K, and Miners JO (2009) Aldosterone glucuronidation by human liver and kidney microsomes and recombinant UDP-glucuronosyltransferases: inhibition by NSAIDs. *Br J Clin Pharmacol* **68:**402–412.

Lash LH, Putt DA, and Cai H (2008) Drug metabolism enzyme expression and activity in primary cultures of human proximal tubular cells. *Toxicology* **244:**56–65.

Little JM, Kurkela M, Sonka J, Jäntti S, Ketola R, Bratton S, Finel M, and Radominska-Pandya A (2004) Glucuronidation of oxidized fatty acids and prostaglandins B1 and E2 by human hepatic and recombinant UDP-glucuronosyltransferases. *J Lipid Res* **45:**1694–1703.

Manevski N, Moreolo PS, Yli-Kauhaluoma J, and Finel M (2011) Bovine serum albumin decreases K_m values of human UDP-glucuronosyltransferases 1A9 and 2B7 and increases V_{max} values of UGT1A9. *Drug Metab Dispos* **39:**2117–2129.

Mazoit JX, Sandouk P, Scherrmann JM, and Roche A (1990) Extrahepatic metabolism of morphine occurs in humans. *Clin Pharmacol Ther* **48:**613–618.

Menochet K, Kenworthy KE, Houston JB, and Galetin A (2011) Simultaneous assessment of uptake and metabolism in rat hepatocytes: a comprehensive mechanistic model. *J Pharmacol Exp Ther* doi:10.1124/jpet.111.187112.

Milne AM, Burchell B, and Coughtrie MW (2011) A novel method for the immunoquantification of UDP-glucuronosyltransferases in human tissue. *Drug Metab Dispos* **39:**2258–2263.

Miners JO, Knights KM, Houston JB, and Mackenzie PI (2006) In vitro-in vivo correlation for drugs and other compounds eliminated by glucuronidation in humans: pitfalls and promises. *Biochem Pharmacol* **71:**1531–1539.

Nishimura M and Naito S (2006) Tissue-specific mRNA expression profiles of human phase I metabolizing enzymes except for cytochrome P450 and phase II metabolizing enzymes. *Drug Metab Pharmacokinet* **21:**357–374.

Ohno S and Nakajin S (2009) Determination of mRNA expression of human UDP-glucuronosyltransferases and application for localization in various human tissues by real-time reverse transcriptase-polymerase chain reaction. *Drug Metab Dispos* **37:**32–40.

Ohtsuki S, Schaefer O, Kawakami H, Inoue T, Liehner S, Saito A, Ishiguro N, Kishimoto W, Ludwig-Schwellinger E, Ebner T, et al. (2012) Simultaneous absolute protein quantification of transporters, cytochromes P450, and UDP-glucuronosyltransferases as a novel approach for the characterization of individual human liver: comparison with mRNA levels and activities. *Drug Metab Dispos* **40:**83–92.

Raoof AA, van Obbergh LJ, de Ville de Goyet J, and Verbeeck RK (1996) Extrahepatic glucuronidation of propofol in man: possible contribution of gut wall and kidney. *Eur J Clin Pharmacol* **50:**91–96.

Rowland A, Gaganis P, Elliot DJ, Mackenzie PI, Knights KM, and Miners JO (2007) Binding of inhibitory fatty acids is responsible for the enhancement of UDP-glucuronosyltransferase 2B7 activity by albumin: implications for in vitro-in vivo extrapolation. *J Pharmacol Exp Ther* **321:**137–147.

Rowland A, Knights KM, Mackenzie PI, and Miners JO (2008) The "albumin effect" and drug glucuronidation: bovine serum albumin and fatty acid-free human serum albumin enhance the glucuronidation of UDP-glucuronosyltransferase (UGT) 1A9 substrates but not UGT1A1 and UGT1A6 activities. *Drug Metab Dispos* **36:**1056–1062.

Rowland A, Knights KM, Mackenzie PI, and Miners JO (2009) Characterization of the binding of drugs to human intestinal fatty acid binding protein (IFABP): potential role of IFABP as an alternative to albumin for in vitro-in vivo extrapolation of drug kinetic parameters. *Drug Metab Dispos* **37:**1395–1403.

Schaefer O, Ohtsuki S, Kawakami H, Inoue T, Liehner S, Saito A, Sakamoto A, Ishiguro N, Matsumaru T, Terasaki T, et al. (2012) Absolute quantification and differential expression of drug transporters, cytochrome P450 enzymes, and UDP-glucuronosyltransferases in cultured primary human hepatocytes. *Drug Metab Dispos* **40:**93–103.

Shipkova M, Strassburg CP, Braun F, Streit F, Gröne HJ, Armstrong VW, Tukey RH, Oellerich M, and Wieland E (2001) Glucuronide and glucoside conjugation of mycophenolic acid by human liver, kidney and intestinal microsomes. *Br J Pharmacol* **132:**1027–1034.

Soars MG, Burchell B, and Riley RJ (2002) In vitro analysis of human drug glucuronidation and prediction of in vivo metabolic clearance. *J Pharmacol Exp Ther* **301:**382–390.

Soars MG, Riley RJ, Findlay KA, Coffey MJ, and Burchell B (2001) Evidence for significant differences in microsomal drug glucuronidation by canine and human liver and kidney. *Drug Metab Dispos* **29:**121–126.

Soars MG, Ring BJ, and Wrighton SA (2003) The effect of incubation conditions on the enzyme kinetics of UDP-glucuronosyltransferases. *Drug Metab Dispos* **31:**762–767.

Soydan AS, Tavares IA, Weech PK, Tremblay NM, and Bennett A (1996) High molecular weight phospholipase A2 and fatty acids in human colon tumours and associated normal tissue. *Eur J Cancer* **32:**1781–1787.

Takizawa D, Hiraoka H, Goto F, Yamamoto K, and Horiuchi R (2005) Human kidneys play an important role in the elimination of propofol. *Anesthesiology* **102:**327–330.

Tsoutsikos P, Miners JO, Stapleton A, Thomas A, Sallustio BC, and Knights KM (2004) Evidence that unsaturated fatty acids are potent inhibitors of renal UDP-glucuronosyltransferases (UGT): kinetic studies using human kidney cortical microsomes and recombinant UGT1A9 and UGT2B7. *Biochem Pharmacol* **67:**191–199.

Tukey RH and Strassburg CP (2000) Human UDP-glucuronosyltransferases: metabolism, expression, and disease. *Annu Rev Pharmacol Toxicol* **40:**581–616.

Address correspondence to: Dr. A. Galetin, School of Pharmacy and Pharmaceutical Sciences, University of Manchester, Stopford Building, Oxford Road, Manchester, M13 9PT, UK. E-mail: aleksandra.galetin@manchester.ac.uk